Received: 7 July 2017 | Revised: 8 November 2017 | Accepted: 18 January 2018

DOI: 10.1111/jvim.15068

STANDARD ARTICLE

Journal of Veterinary Internal Medicine Open Access

ACVIM American College of Veterinary Internal Medicine

Comparative, multidimensional imaging of patent ductus arteriosus and a proposed update to the morphology classification system for dogs

Kelley R. Doocy | Ashley B. Saunders | Sonya G. Gordon | Nicholas Jeffery

Department of Small Animal Clinical Sciences, College of Veterinary Medicine and Biomedical Sciences, Texas A&M University, College Station, Texas

Correspondence
Dr Ashley B. Saunders, Department of Small Animal Clinical Sciences, College of Veterinary Medicine and Biomedical Sciences, Texas A&M University, College Station, TX 778434474.
Email: asaunders@cvm.tamu.edu

Funding information
Frankie's Friends Charitable Pet Foundation; The Ginn Fund, Texas A&M University

Background: Accurately assessing the morphology and shape of the patent ductus arteriosus (PDA) and obtaining measurements are important to avoid procedural complications.

Objectives: To characterize and compare PDA morphology, shape, and dimensions with angiography and echocardiography.

Animals: 25 client-owned dogs with echocardiographically confirmed PDA.

Methods: Prospective case series. Imaging consisted of single plane angiography, transthoracic echocardiography from the right (TTE-R) and left (TTE-L), and two-dimensional, biplane, and three-dimensional transesophageal echocardiography (TEE-2D and TEE-3D). Measurements included angiographic minimal ductal diameter (MDD), echocardiographic pulmonary ostium in a single dimension (TTE-R, TTE-L, and TEE-2D) and in perpendicular dimensions (TEE-3D) with similar measurements of the ampulla 3 mm above the MDD or pulmonary ostium. The morphology and shape of the PDA were characterized.

Results: Catheter-based occlusion ($N = 20$) and surgical ligation ($N = 5$) were performed without complication. Angiographic morphology was classified as type II ($N = 19$), type III ($N = 1$), and other ($N = 1$). Angiographic MDD and TEE-2D pulmonary ostium measurements were significantly ($P = .008$) but weakly correlated ($r = .56$); similar relationships were found for ampulla diameter measurements ($P < .0001$; $r = .75$). In general, TEE-2D did not correlate with other imaging modalities measurements. Based on TEE-3D measurements, the majority of pulmonary ostium (17/24; 71%) and ampulla (19/24; 79%) were oval.

Conclusions and Clinical Importance: Measurements using different imaging modalities are not interchangeable. TEE-3D provided an en face view of the PDA that cannot be replicated with other echocardiographic techniques and demonstrated an oval shape in the majority of dogs. We propose an update to the current classification system to include additional PDA morphologies.

KEYWORDS

angiography, canine, congenital heart disease, echocardiography, three-dimensional

Abbreviations: 2D, two-dimensional; 3D, three-dimensional; L, left; MDD, minimal ductal diameter; PA, pulmonary artery; PDA, patent ductus arteriosus; R, right; TEE, transesophageal echocardiography; TTE, transthoracic echocardiography.

Presented as an abstract at the 2017 American College of Veterinary Internal Medicine Forum, National Harbor, Maryland.

The work was done at Texas A&M University.

1 | INTRODUCTION

Definitive closure of patent ductus arterious (PDA) in dogs includes catheter-based occlusion with the canine-specific, Amplatz Canine Duct Occluder (ACDO; Infiniti Medical, LLC, Menlo Park, California).[1,2] The procedural objective is complete occlusion without complications. Although procedural success is reportedly high, residual flow, and device embolization have been described with the ACDO and are likely underrepresented in the literature).[1–5] Additionally, it is important to identify PDA morphologies that are not amenable to closure with the ACDO device.[6,7]

Abnormal distribution of ductal wall muscle and replacement by elastic tissue has been documented by histopathology of PDA in dogs[8,9] and results in a wide range of PDA sizes and morphologies. Individual variations in PDA morphology, PDA size, and arterial size for vascular access influence closure recommendations and device selection. Therefore, accurate assessment of PDA morphology and size are important for device selection and optimal device sizing to avoid complications. Morphologic description and device sizing recommendations are typically based on angiographic characterization of the minimal ductal diameter (MDD) and ampulla of the PDA.[10–12] With angiography, the MDD is obtained by measuring the contrast jet as it flows from the PDA ampulla into the pulmonary artery (PA). Echocardiographic assessment of the PDA can provide additional information. With echocardiography, the tissue of the ampulla and pulmonary ostium of the ductus arteriosus is typically visualized and measured. Color Doppler can assist in identifying the PDA but measurements of the color signal can overestimate the PDA size.[13,14] Measurements acquired with transthoracic echocardiography (TTE) were reportedly not interchangeable with angiographic measurements based on wide limits of agreement when comparing the two modalities.[1] Transesophageal echocardiography (TEE) has reported benefits including the potential of superior imaging compared with TTE as well as real-time monitoring of the procedure in two- and three-dimensions (2D, 3D).[4,6,15,16] Intraoperative imaging with TEE can alter treatment decisions that were originally based on angiographically derived measurements.[6,17] A similar finding in people has been reported.[18–20] Images obtained with multiplane TEE demonstrate variations in cross-sectional shape of the PDA.[4,6,17] The objective of this study was to characterize PDA shape and dimensions using single plane, right lateral angiography, and echocardiography including TTE from the right (TTE-R) and left (TTE-L) and TEE in 2D, biplane, and 3D. We hypothesized that an oval shaped PDA is more common than previously reported and that 3D imaging in particular would provide the most detailed information.

2 | ANIMALS, MATERIAL, AND METHODS

This study was approved by the Institutional Animal Care and Use Committee and the Clinical Research and Review Committee at Texas A&M University. Owner consent was obtained for all dogs.

Client-owned dogs weighing $>$2.0 kg with echocardiographically confirmed left-to-right shunting PDA were eligible to participate. Very small dogs in which the TEE probe (4D TEE transducer, GE Vingmed Ultrasound, AS Standpromenaden 45 N-3191, Horten, Norway) would not pass down the esophagus were excluded. In an attempt to include a variety of PDA morphologies, the study was designed to enroll 20 dogs scheduled for a catheter-based occlusion procedure and 5 for surgical ligation. All dogs had a complete TTE study (GE Vivid E9 with XDclear, GE Vingmed Ultrasound, AS Standpromenaden 45 N-3191, Horten, Norway) performed with an appropriately selected 3.5–12 MHz phased-array transducer. Cineloops of the PDA were obtained from the right parasternal short axis view at the level of the main PA and the left parasternal cranial short axis view. Based on the morphology of the PDA and the weight of the dog, which could limit vascular access in small dogs, catheter-based occlusion or surgical ligation was recommended and performed the next day. After anesthetic induction, a complete TEE study was performed to visualize the PDA in 2D and multiplane (biplane and 3D) views. For biplane TEE imaging, the image was oriented so that the cursor crossed the ampulla in a plane that was perpendicular. For 3D TEE, the image was rotated until the PDA was visualized en face looking down the ampulla towards the PA and the cursor was translated down into the ampulla to display the aorta (right), PDA (middle), and PA (left) in cross section (Figure 1E). In the 2D reference images for TEE-3D, the display order is aorta (top), PDA (middle), and PA (bottom). Dogs scheduled for catheter-based occlusion had a right lateral angiogram performed via the right femoral artery as previously described.[2] Cineloop images from the TTE, TEE, and angiographic studies were stored and saved for offline analysis (EchoPAC v201; GE Medical Systems, Horten, Norway; eFilm version 3.3.0, Sound-Eklin, Carlsbad, California). At the time of the procedure, acquired images were used real-time for decisions made by the attending cardiologist regarding device selection, sizing, and completeness of closure. Device type, size, and any procedural complications were recorded. All dogs underwent a complete TTE study the next day before discharge, and the presence of residual ductal flow was recorded.

Once all dogs had completed the study, images were reviewed by two investigators (KRD, ABS) and the optimal image of the PDA in each imaging modality (TTE-R, TTE-L, TEE-2D, TEE-3D, and angiogram) was selected and stored. The optimal image was defined as the image that displayed the site of the smallest diameter at its maximum size. After calibration, measurements of the angiographic MDD were made at each edge of the contrast stream (Figure 1) and measurements of the TTE/TEE pulmonary ostium were made inner edge to inner edge in a single plane for TTE taking care to distinguish the pulmonary ostium from the left PA especially in TTE-R images (Figure 2), and TEE-2D and in two planes (A and B) for TEE-3D (Figure 1). "A" represents the minor axis perpendicular to the PA between the PA and aorta and "B" represents the major axis 90° to "A" (Figure 1E,F). The diameter of the ampulla was measured 3 mm above the MDD or pulmonary ostium in a single plane for TTE and TEE-2D and in two planes (A and B) for TEE-3D (Figure 1) to approximate the location of the ACDO proximal disk. With TEE-3D imaging, a dynamic change in the PDA throughout the cardiac cycle can be observed (Supporting Information Video 1). The optimal image was selected where the ampulla and pulmonary

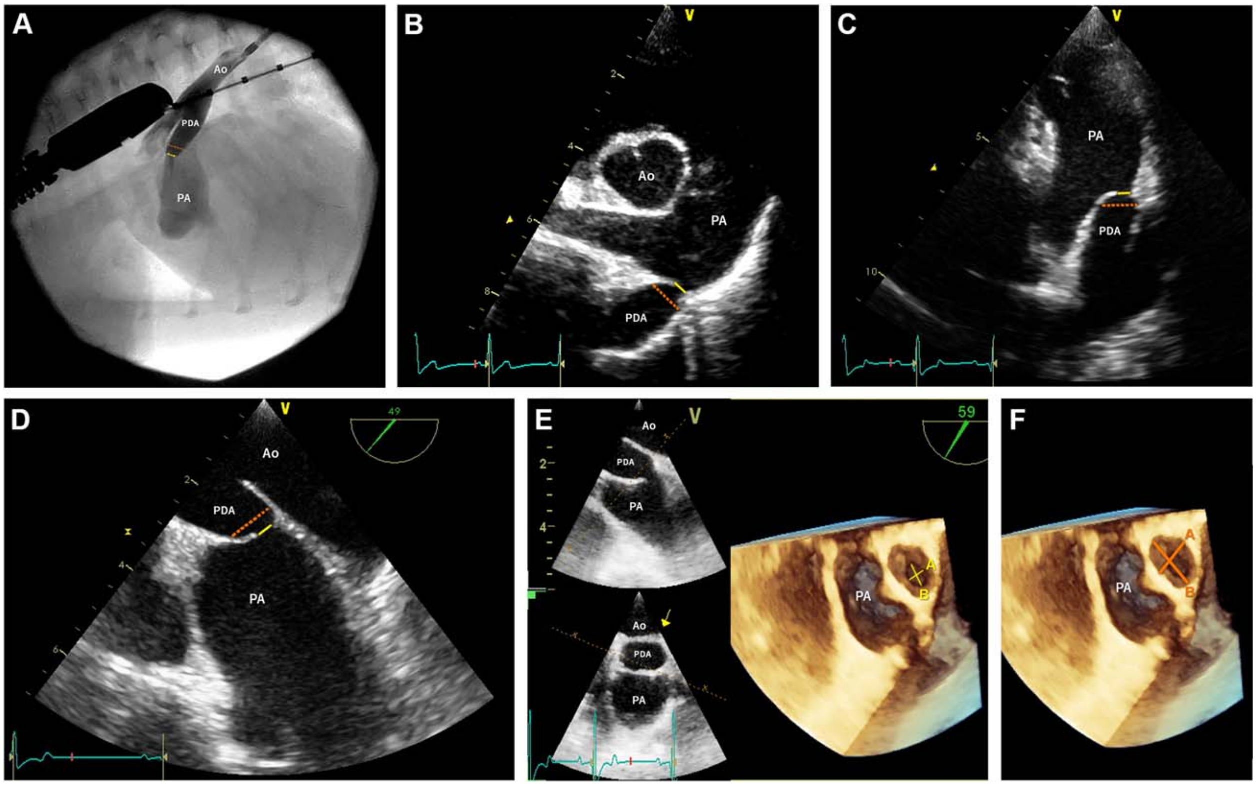

FIGURE 1 Measurements of the MDD or pulmonary ostium (yellow line) and ampulla (orange line) of the PDA for (A) lateral angiogram, (B) transthoracic echocardiographic image from the right (TTE-R), (C) transthoracic echocardiographic image from the left (TTE-L), (D) transesophageal echocardiographic image in 2D (TEE-2D), (E,F) transesophageal echocardiographic image in 3D (TEE-3D) with perpendicular measurements A (minor axis) and B (major axis) of the pulmonary ostium (E) and ampulla (F) with the 2D reference images included. Ao, aorta; PA, pulmonary artery

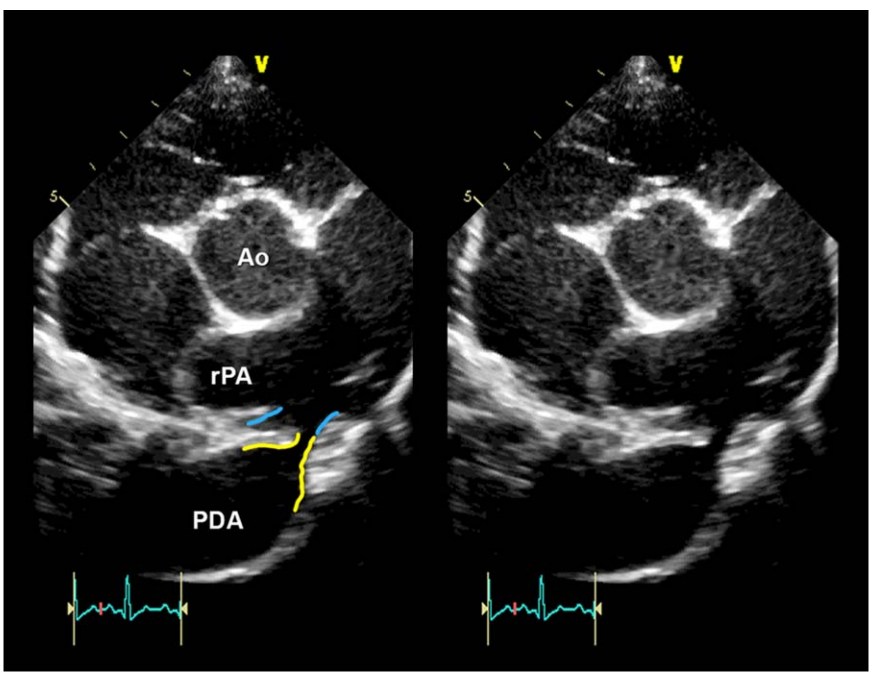

FIGURE 2 Transthoracic echocardiographic image obtained in a right parasternal short axis basilar view to demonstrate the difference between the location of the left branch PA (outlined in blue) and pulmonary ostium of the PDA (outlined in yellow). Ao, aorta; rPA, right branch PA

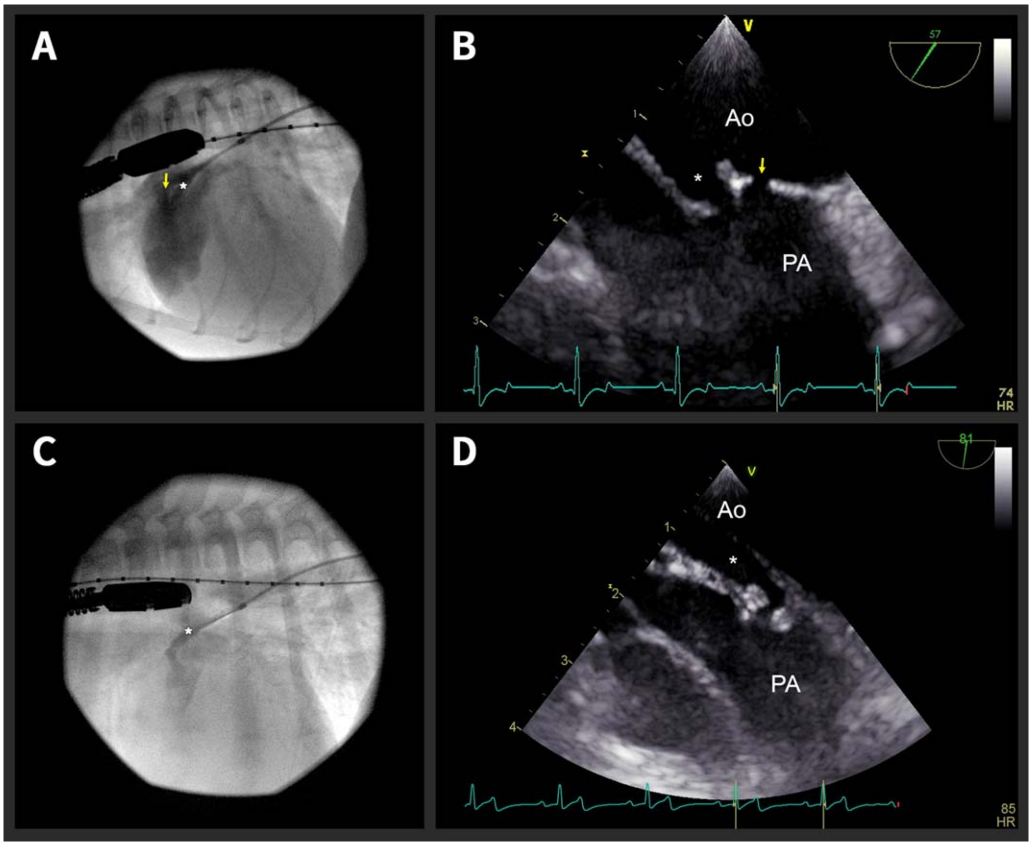

FIGURE 3 Example angiographic and TEE images where TEE provided additional information to guide treatment decisions. (A,B) The patent ductus arteriosus (PDA*) does not taper and an additional communication (aortopulmonary window, arrow) is present between the aorta (Ao) and PA cranial to the PDA. (C,D) The PDA (*) has excessive tissue on the PA side

ostium were clearly visible and the timing in the cardiac cycle was recorded based on review of the simultaneous ECG.

The TEE-3D A and B measurements were used to determine the shape of the pulmonary ostium and ampulla. The shape was categorized as circular (difference in A and B $\leq$ 0.5 mm) or oval (difference in A and B $>$ 0.5 mm). Of note, the term elliptical has been used in the canine literature.[4,6,17] We elected to use the term oval in this study to encompass all shapes that are not circular including an ellipse. An ellipse indicates the distance between two focal points remains constant whereas an oval can vary in shape.[21] Angiographic classification of the PDA was assigned based on Miller's description in dogs.[10]

3 | STATISTICAL ANALYSIS

Descriptive statistics were calculated. The D'Agostino-Pearson test was used to verify normal distribution of variables. The angiographic measurements were not normally distributed therefore measurements are reported as median and range. Ductal MDD (or pulmonary ostium) and ampulla measurements were evaluated with Pearson's correlation coefficient and compared by Bland-Altman analysis.[22] For each imaging modality, individual measurements for each dog were compared with the same dog's TEE-2D measurements and plotted with line graphs. Statistical analyses were performed using commercial software (GraphPad Prism 7 for Windows, GraphPad Software, La Jolla, California). A P value $<$ .05 was considered significant.

4 | RESULTS

4.1 | General characteristics of the study population

Twenty-five dogs with echocardiographic confirmation of left-to-right shunting PDA were enrolled. The median age was 12 months (range, 3–72 months), and median weight was 7.6 kg (range, 2.3–36.8 kg). The majority were female (19/25, 76%). Breeds included mixed (n = 6) and 2 each of Yorkshire Terrier, Labrador Retriever, Chihuahua, German Shepherd, Schnauzer, and English Springer Spaniel. Remaining breeds included one of each of the following: Miniature Poodle, Pomeranian, Maltese, Bichon Frise, Weimaraner, and Shih Tzu. As planned, 20 dogs had a catheter-based occlusion procedure and 5 underwent surgical ligation. Ligation was recommended in 3 dogs that were too small for a catheter-based occlusion procedure and in 2 dogs in which the PDA morphology was tubular and not amenable to catheter-based occlusion. In one of these 2 dogs, angiography suggested multiple aorta to PA communications and surgery was recommended based on the simultaneous TEE images providing additional anatomical information including a short, tubular ductal morphology, and the second communication between the aorta and main PA consistent with an aortopulmonary window cranial to the PDA (Figure 3A,B and Supporting Information

TABLE 1 Patent ductus arteriosus measurements in dogs

	Angiograhy (mm)	TTE-R (mm)	TTE-L (mm)	TEE-2D (mm)	TEE-3D (mm)
Angiographic MDD/Echocardiographic pulmonary ostium	3.0 (1.8–4.8)	4.2 (1.5–8.1)	3.2 (2.0–4.5)	3.0 (1.3–5.7)	A: 2.1 (0.4–3.6) B: 3.1 (0.9–5.8)
Ampulla	8.1 (3.2–11.3)	9.1 (4.5–13.0)	8.7 (3.5–12.1)	7.6 (4.0–14.8)	A: 5.7 (1.4–8.3) B: 7.6 (2.6–11.8)

Abbreviations: MDD, minimal ductal diameter; L, left; R, right; TTE, transthoracic echocardiography; TEE, transesophageal echocardiography; 2D, two-dimensional; 3D, three-dimensional.
Data reported as median (range).

Video 2). This was the only dog that had a ligation and an angiographic study. In the 21 dogs for whom angiography was performed, morphology was classified as type IIA (n = 16), type IIB (n = 3), type III (n = 1, subsequently ligated), and other (n = 1, similar to Krichenko type D, Figure 3C,D, and Supporting Information Video 2).[23]

4.2 | Ductal measurements

Ductal measurements were obtained from each imaging modality and are reported in Table 1. Individual measurements for the angiographic MDD and echocardiographic pulmonary ostium are displayed in Figure 4. There was significant, but weak, correlation between angiographic MDD and TEE-2D pulmonary ostium measurements ($r = .56$, $P = .008$) in this study population (Figure 5A). This was explored further with Bland-Altman analysis (Figure 5). Figure 5B-F shows the Bland-Altman analysis for TEE-2D measurements compared to measurements from the other modalities (angiography, TTE-R, TTE-L, TEE-3D A, and TEE-3D B). The TEE-2D measurement was selected for comparison because it typically provides a complete image of the PDA. The limits of agreement were wide for each modality. Notably, the TTE-R measurements of the MDD systematically overestimate the TEE-2D pulmonary ostium measurements by up to 4.0 mm (>1.0 mm in 13/25 [52%]) (Figure 5C). On Bland-Altman plots, the TEE-3D B diameter measurements appeared to be the most similar to TEE-2D measurements with the least bias; however, when the two measurements for each dog were plotted individually on a line graph (Figure 6), the measurements made by the 2 methods differed by as much as 2.5 mm. In one dog that had a surgical ligation performed, TEE-3D was not obtained because the image quality was adversely affected by air entering the thorax. When compared with TEE-2D and TEE-3D B, the TEE-3D A measurements were consistently smaller (Figure 4).

Angiographic and TEE-2D ampulla measurements were significantly, but only moderately, correlated ($r = .75$, $P < .0001$; Figure 7A). As with the pulmonary ostium measurements, Bland-Altman analysis was performed for each modality (angiography, TTE-R, TTE-L, TEE-3D A, and TEE-3D B) compared with TEE-2D (Figure 7). The limits of agreement were wide for each modality. Notably, TTE-R and TTE-L measurements were consistently larger than those derived by TEE-2D measurements.

4.3 | Ductal characteristics and shape

For the 24 dogs in which TEE-3D was performed, the optimal image of the PDA used in the analysis was obtained during diastole (23/24) and systole (1/24). Systolic measurements were selected as the ideal image in one dog with an unusual PDA morphology (Figure 3C,D) that did not readily fit into Miller's classification scheme.[10] Of note, the pulmonary ostium in this dog was at an angle best visualized with TEE-3D, thus

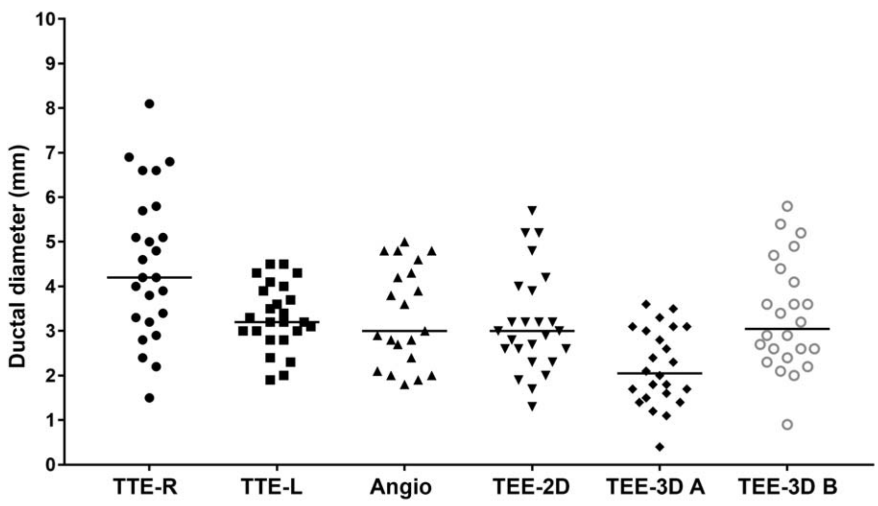

FIGURE 4 Dot plot of angiographic MDD and echocardiographic pulmonary ostium measurements. The solid line represents the median. TEE, transesophageal echocardiography; TTE, transthoracic echocardiography; R, right; L, left; 2D, two-dimensional; 3D, three-dimensional

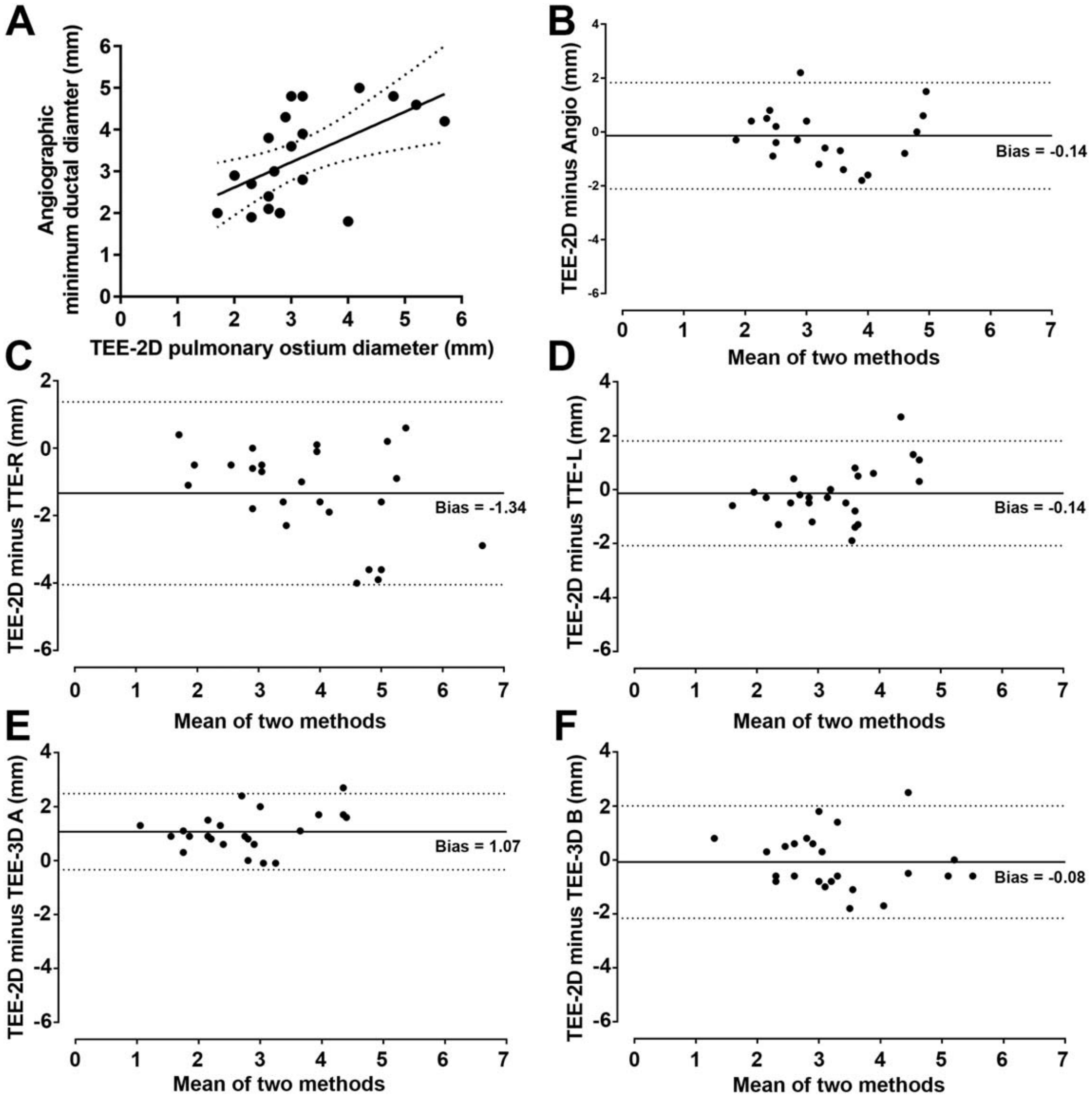

FIGURE 5 (A) Correlation between angiographic MDD and TEE-2D pulmonary ostium measurements; (B-F) Bland-Altman plots for TEE-2D pulmonary ostium measurements compared to (B) angiographic MDD, (C) TTE-R, (D), TTE-L, (E) TEE-3D A; and (F) TEE-3D B. Dashed lines represent 95% limits of agreement and solid line represents the mean bias

this dog's measurements represent the outlying lowest value for TEE-3D A and B in Figure 4. When comparing the TEE-3D A and B dimensions for the pulmonary ostium and ampulla, A was smaller than B in 23/24 (96%; 1 dog A = B) for the pulmonary ostium (Figure 8) and 20/24 (83.3%; 3 dogs A = B; 1 dog A > B) for the ampulla. The majority of dogs had an oval shape pulmonary ostium (17/24; 71%, Supporting Information Video 1) and ampulla (19/24; 79%). The 7 dogs with a circular-shaped pulmonary ostium were all classified with a Type IIA PDA morphology on angiography, and the TEE-3D B diameter of the circles was below 4 mm, ranging in size from 0.9, 2.2, 2.4, 2.6, 2.9, 3.2, and 3.6 mm. The shape combinations for the pulmonary ostium/ampulla in which O denotes an oval and C denotes a circular shape included O/O in 16, O/C in 1, C/O in 3, and C/C in 4.

When performing biplane TEE imaging, we observed that it was difficult to consistently and accurately place the cursor across the ampulla in a manner that did not create an oblique angle. For this reason, we did not include these measurements in the final analysis and caution their use in making an assessment of circular or oval shape. The reference 2D image can help the operator determine if the cursor crosses perpendicular or at an oblique angle.

4.4 | Device characteristics

Median ACDO size for 20 dogs in which a device was placed was 7 (range, 3–10). Median ACDO to MDD ratio was 2.0 (range, 1.5–3.2) with angiography, and ACDO to pulmonary ostium ratio was 2.1 (range, 1.4–3.3) with TEE-2D, 3.1 (range, 1.4–7.5) with TEE-3D A, and 2.0 (range, 1.1–3.4) with TEE-3D B. Median ACDO proximal disc to ampulla ratio was 1.7 (range, 1.3–2.8) with angiography, 1.7 (range, 1.1–2.6) with TEE-2D, 2.2 (range, 1.4–7.5) with TEE-3D A, and 1.6 (range, 1.1–4.0) with TEE-3D B. Based on TEE-2D and angiographic imaging, the median oversize factor for the ACDO to pulmonary ostium was similar to ratios previously reported (median 2.0 depending on imaging modality used to select a device in an individual dog), and the

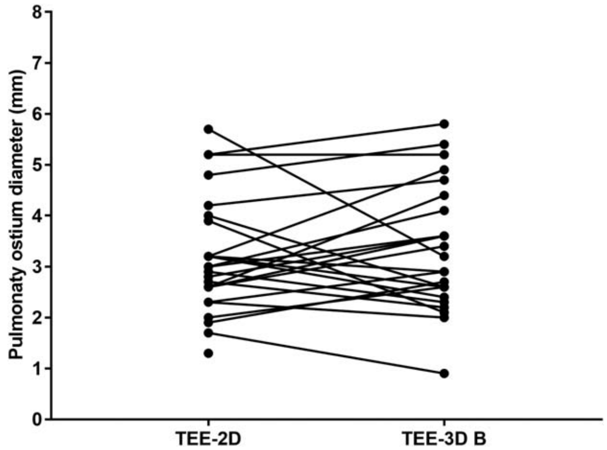

FIGURE 6 Line graph comparing pulmonary ostium measurements from TEE-2D and TEE-3D B for each dog to demonstrate the measurements were highly variable despite Bland-Altman analysis suggesting they had the "best" comparison with the least bias. In one dog that had a surgical ligation performed, TEE-3D was not obtained because the image quality was adversely affected by air entering the thorax. The dog is represented with only a TEE-2D measurement

proximal disc to ampulla diameter ratio was always > 1. No complications occurred in any dog and there was no residual flow on TTE before discharge.

5 | DISCUSSION

The results of this study provide additional information regarding 3D morphology of PDA in dogs. Earlier reports suggested on oval-shaped PDA can occur in dogs, which is not surprising based on histopathologic appearance of the PDA and variability in ductal wall muscle tissue.[6,8,9] Angiography and TTE display a 2D image of the PDA and does not readily demonstrate the variation in cross sectional shape (ie, circular, oval). In this study, TEE-3D provided unique information regarding overall shape and measurements ("A" and "B") by displaying the pulmonary ostium of the PDA en face. We evaluated the shape of the ampulla and pulmonary ostium to demonstrate that there are a variety of shape combinations with the majority (71%) of dogs in this study identified as having an oval-shaped pulmonary ostium. This is much higher than in a previous study in which 5 of 80 dogs (6%) were reported to have an elliptical shaped ostium based on TEE-2D imaging.[17] Biplane TEE images from 2D can be difficult to align in a perpendicular plane directly through the pulmonary ostium, resulting in an obliqued view and a false impression of the ductal shape and size. A noncircular shape could lead to differences in diameter measurements between imaging modalities depending on the location and angle in which the image of the PDA was obtained.

Historically, single plane lateral angiography was used to create the current PDA morphology classification system in dogs,[10] and angiographic measurements are the basis for sizing recommendations in the original reports of the ACDO device.[1,11] Subsequent reports using the ACDO included ampulla diameter measurements from angiography and echocardiography compared with the device proximal disk dimension when selecting device size.[2,17] Ductal measurements tend to vary between imaging modalities. Characterizing solely based on single plane angiography may not always be adequate[10] particularly when contrast is delivered by a hand injection in large dogs or in large, high flow PDA, and TTE can be limited by image quality and overestimates of size.[1,7,17] It is important to consider that TTE has consistently been shown to overestimate angiographic measurements in other studies[1,17] and TEE measurements in our study. Comparisons in our study were made to the TEE-2D measurements because TEE-2D provides direct visualization of the walls of the PDA extending from aorta to the pulmonary ostium. In our study, TEE identified dogs with unusual ductal anatomy (Figure 3) and helped guide next steps for successful closure. Whereas, measurements can statistically appear to relate well between modalities when looking at the study population that includes all dogs, the individual comparison of measurements by different techniques in an individual dog shows the absolute values are different and are not always interchangeable. This could be related to the variation in PDA shape, change throughout the cardiac cycle, and angle in which each image and therefore measurement is obtained. In one study, the difference between TTE and TEE measurements would have resulted in devices that differed by up to 2 sizes in 17/80 (21%) of the dogs.[17] Ultimately, small differences in measurements are unlikely to alter the procedure or outcome but large differences could be important and affect device selection and sizing.

The ACDO is made up of two circular-shaped disks (one flat, one cupped) separated by a waist and constructed of nitinol mesh designed to conform to the ampulla of the PDA when deployed.[12] In dogs, sizing issues are reported resulting in the device not assuming its native shape after deployment, residual flow through or around the device, and device embolization.[1,4,7,17] Avoiding undersizing is important because the PDA can increase in size after occlusion,[1] which is one possible cause for device embolization in the authors' experience.[24] Therefore, obtaining accurate anatomic information is valuable for avoiding complications with the procedure.

Some dogs in this study had ductal anatomy that did not readily fit into the current classification scheme. Successful ductal occlusion in this study was achieved in part as a result of information gained with intraoperative TEE imaging. The PDA classification scheme in humans includes a larger range of morphologies than dogs that is based on location (ie, pulmonary, mid ampulla, or aorta) of the narrowest part of the PDA and includes groups with multiple constrictions or unusual/unique morphologies.[23] With advancements in 3D imaging and as TEE probes become more readily available in veterinary medicine, updates to both the current morphology classification to include additional morphologies and angiographic based sizing guidelines to include TEE assessment of multidimensional anatomy, shape, and ampulla diameter may help to further minimize or avoid complications. We propose the addition of two categories to the current 3 (type I, II, III) to include those with multiple narrowings at various levels (type IV, similar to type D[25]) and other unusual morphologies (type V, Figure 3), both of which have been encountered by the authors, to recognize that there are dogs with PDA morphologies that do not fit in the current classification

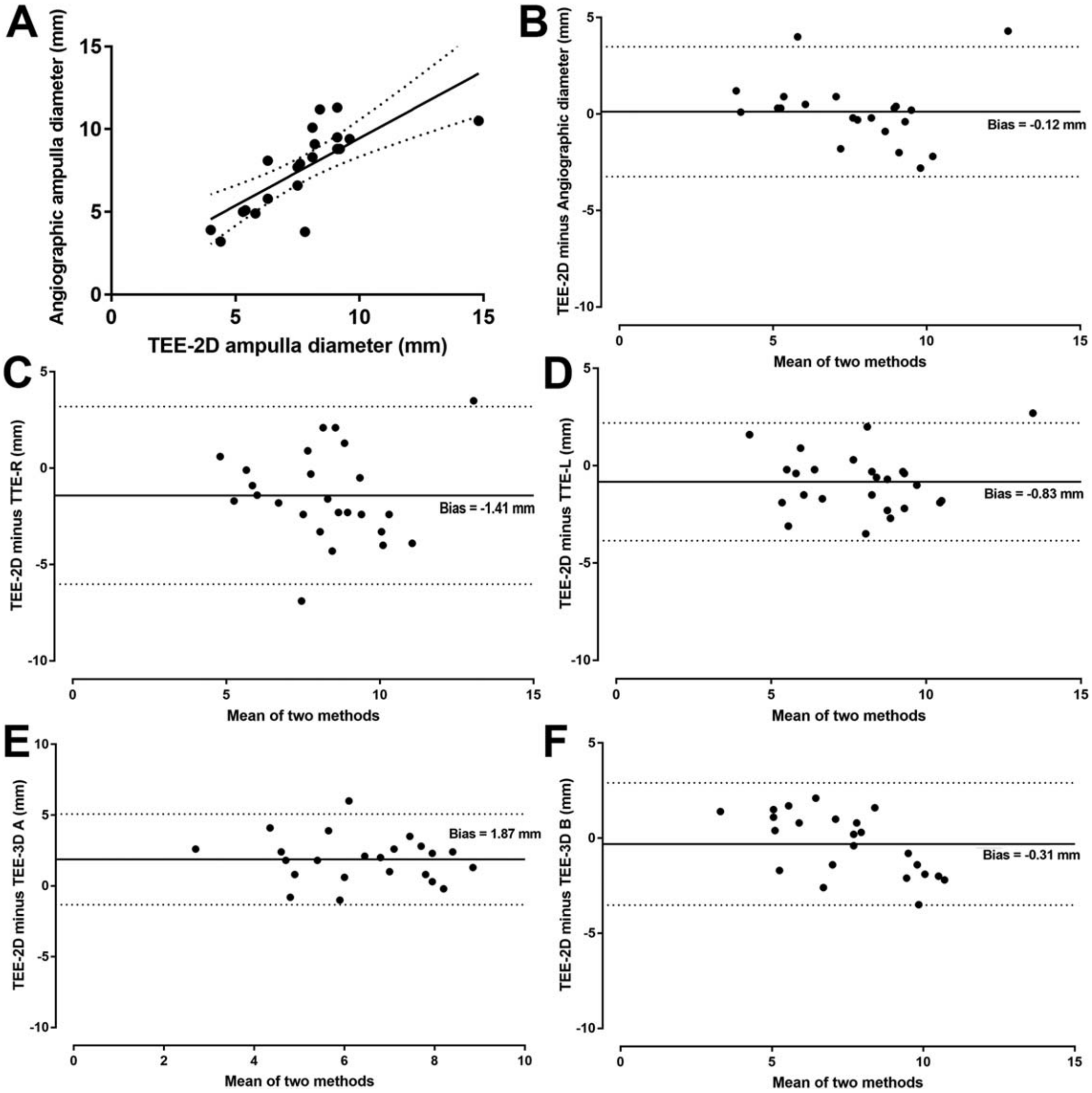

FIGURE 7 (A) Correlation between angiographic and TEE-2D ampulla measurements; (B-F) Bland-Altman plots for TEE-2D ampulla measurements compared to (B) angiographic, (C) TTE-R, (D) TTE-L, (E) TEE-3D A, and (F) TEE-3D B. Dashed lines represent 95% limits of agreement and solid line represents the mean bias

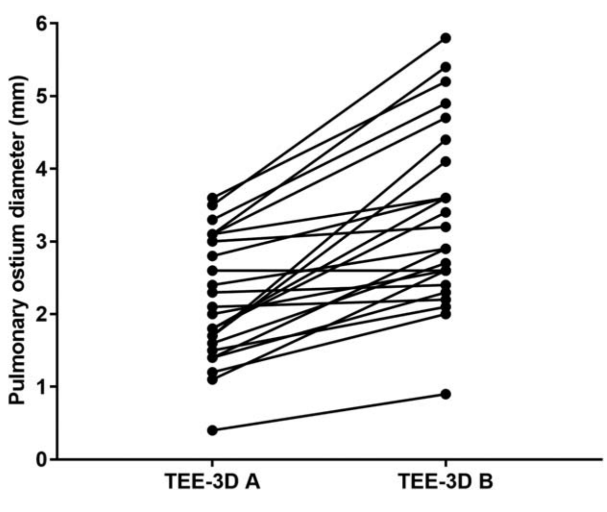

FIGURE 8 Line graph comparing TEE-3D A and B pulmonary ostium measurements for each dog to demonstrate circular or oval shape

scheme and may require additional imaging and procedural planning for a successful outcome. An oval shape was not more likely to occur in any one type of ductal morphology in this study, and we did not identify specific factors in other imaging modalities (ie, angiography, TTE-2D, or TEE-2D) that would have indicated an oval shape with 3D imaging. More detailed information about shape and dimensions obtained with TEE may be of value particularly in complicated cases with unusual ductal morphology or in situations where less experienced operators are performing the procedure. As we have recently reported, training and confidence levels when performing ductal occlusion vary.[26]

This study has several limitations. Measurements are not compared with gross specimens to confirm accuracy. Therefore, it is not possible to know which modality is truly most accurate. This is a small study; but despite this limitation, we were able to include a variety of PDA morphologies. The majority of ductal morphologies are Type II but other morphologies do occur and proper imaging is essential for guiding management decisions. Although there are clear benefits of TEE, it requires purchase of a specialized probe, experienced operators to perform the study during the procedure and cannot always be used in very small dogs. At our institution, TEE is performed in some dogs during surgical ligation to confirm closure although air interface can adversely affect image quality as occurred in one dog in this report.

In conclusion, TEE-3D provides a unique view of the PDA that cannot be replicated with other echocardiographic techniques or single plane angiography. We demonstrated that the majority of dogs in this study had an oval not circular-shaped PDA and that the PDA changes throughout the cardiac cycle. A noncircular shape could lead to differences in diameter measurements between imaging modalities depending on the location and angle the image was obtained which is one possible reason for the weak correlation between angiographic and echocardiographic measurements. We recognize that small differences in measurements might not be important but large differences could affect treatment decisions and result in procedural complications. This morphologic information may be useful for device sizing and future development of devices. We also encountered PDA morphologies that did not fit into the current classification scheme suggesting an updated scheme would be useful. Our recommendations for making procedural decisions and selecting device size are to use the measurements from the highest quality image and to be cautious making decisions based on measurements from images that do not clearly delineate the PDA.

ACKNOWLEDGMENTS

The authors thank Jill VanWhy and Kathy Glaze for their technical support, Scott Birch for figure preparation, Dr Noah Cohen for his expert advice, and Drs Geni Bermes, Bruno Boutet, Justin Carlson, Nicole Culwell, Crystal Hariu-Damore, Marty Henderson, Brooke Knowlton, Katie Meier, Kelly Nitsche, and Jordan Vitt for their support and assistance with case management.

CONFLICT OF INTEREST DECLARATION

Authors declare no conflict of interest.

OFF-LABEL ANTIMICROBIAL DECLARATION

Authors declare no off-label use of antimicrobials.

INSTITUTIONAL ANIMAL CARE AND USE COMMITTEE (IACUC) OR OTHER APPROVAL DECLARATION

This study was approved by the IACUC and the Clinical Research and Review Committee at Texas A&M University.

ORCID

Ashley B. Saunders http://orcid.org/0000-0001-9908-3894

REFERENCES

[1] Nguyenba TP, Tobias AH. Minimally invasive per-catheter patent ductus arteriosus occlusion in dogs using a prototype duct occluder. *J Vet Intern Med.* 2008;22:129–134.

[2] Gordon SG, Saunders AB, Achen SE. Transarterial ductal occlusion using the Amplatz canine duct occluder in 40 dogs. *J Vet Cardiol.* 2010;12:85–92.

[3] Carlson JA, Achen SA, Saunders AB, et al. Delayed embolization of an Amplatz canine duct occluder in a dog. *J Vet Cardiol.* 2013;15: 271–276.

[4] Porciello F, Caivano D, Giorgi ME, et al. Transesophageal echocardiography as the sole guidance for occlusion of patent ductus arteriosus using a canine ductal occluder in dogs. *J Vet Intern Med.* 2014; 28:1504–1512.

[5] Gordon, S. G., Saunders, A. B., Fries, R., & Rishniw, M. Complications associated with transcatheter PDA occlusion: results of an ACVIM cardiology survey. In: Proceedings American College of Veterinary Internal Medicine Forum; June 2014; Nashville, TN.

[6] Saunders AB, Achen SE, Gordon SG, Miller MW. Utility of transesophageal echocardiography for transcatheter occlusion of patent ductus arteriosus in dogs: influence on the decision-making process. *J Vet Intern Med.* 2010;24:1407–1413.

[7] Caivano D, Birettoni F, Fruganti A, et al. Transthoracic echocardiographically-guided interventional cardiac procedures in the dog. *J Vet Cardiol.* 2012;14:431–444.

[8] Buchanan JW. Morphology of the ductus arteriosus in fetal and neonatal dogs genetically predisposed to patent ductus arteriosus. *Birth Defects Orig Artic Ser.* 1978;14:349–360.

[9] Buchanan JW. Patent ductus arteriosus morphology, pathogenesis, types and treatment. *J Vet Cardiol.* 2001;3:7–16.

[10] Miller MW, Gordon SG, Saunders AB, et al. Angiographic classification of patent ductus arteriosus in the dog. *J Vet Cardiol.* 2006;8: 109–114.

[11] Nguyenba TP, Tobias AH. The Amplatz canine duct occluder: a novel device for patent ductus arteriosus occlusion. *J Vet Cardiol.* 2007;9:109–117.

[12] Amplatz® Canine Duct Occluder. Amplatz® Canine Duct Occluder Instruction Manual. http://www.infinitimedical.com/wpcontent/uploads/2013/05/ampltaz.pdf. Accessed June 30, 2017.

[13] Saunders AB, Miller MW, Gordon SG, Bahr A. Echocardiographic and angiographic comparison of ductal dimensions in dogs with patent ductus arteriosus. *J Vet Intern Med.* 2007;21:68–75.

[14] Schneider M, Hildebrandt N, Schweigl T, et al. Transthoracic echocardiographic measurement of patent ductus arteriosus in dogs. *J Vet Intern Med.* 2007;21:251–257.

[15] Pariaut R, Moise NS, Kraus MS, et al. Use of transesophageal echocardiography for visualization of the patent ductus arteriosus during transcatheter coil embolization. *J Vet Cardiol.* 2004;6: 32–39.

[16] Doocy KR, Nelson DA, Saunders AB. Real-time 3D transesophageal echocardiography-guided closure of a complicated patent ductus arteriosus in a dog. *J Vet Cardiol* 2017;19:287–292.

[17] Silva J, Domenech O, Mavropoulou A, et al. Transesophageal echocardiography guided patent ductus arteriosus occlusion with a duct occluder. *J Vet Intern Med.* 2013;27:1463–1470.

[18] Gologorsky E, Gologorsky A, Barron ME, Salerno TA. Patent ductus arteriosus revisited: myths and misconceptions. *Anesth Anal.* 2011; 113:425.

[19] Shyu K-G, Lai L-P, Lin S-C, et al. Diagnostic accuracy of transesophageal echocardiography for detecting patent ductus arteriosus in adolescents and adults. *Chest.* 1995;108:1201–1205.

[20] Takenaka K, Sakamoto T, Shiota T, et al. Diagnosis of patent ductus arteriosus by biplane color Doppler flow mapping. *Am J Cardiol.* 1991;68:691–693.

[21] Encyclopedia of Mathematics. Oval, Encyclopedia of Mathematics. https://www.encyclopediaofmath.org//index.php?title=Oval&oldid=31013. Accessed March 28, 2017.

[22] Bland JM, Altman DG. Statistical methods for assessing agreement between two methods of clinical measurement. *Lancet*. 1986;1:307–310.

[23] Krichenko A, Benson LN, Burrows P, et al. Angiographic classification of the isolated, persistently patent ductus arteriosus and implications for percutaneous catheter occlusion. *Am J Cardiol*. 1989;63:877–880.

[24] Wesselowski S, Saunders AB, Gordon SG. Relationship between device size and body weight in dogs with patent ductus arteriosus undergoing Amplatz canine duct occluder deployment. *J Vet Intern Med*. 2017;17:192–194.

[25] Schneider M, Schneider I, Hildebrandt N, Wehner M. Percuatneous angiography of patent ductus arteriosus in dogs: techniques, results and implications for intravascular occlusion. *J Vet Cardiol*. 2003;5:21–27.

[26] Saunders AB, Keefe L, Birch SA, et al. Perceptions of transcatheter device closure of patent ductus arteriosus in veterinary cardiology and evaluation of a canine model to simulate device placement: a preliminary study. *J Vet Cardiol*. 2017;19:268–275.

SUPPORTING INFORMATION

Additional Supporting Information may be found online in the supporting information tab for this article.

How to cite this article: Doocy KR, Saunders AB, Gordon SG, Jeffery N. Comparative, multidimensional imaging of patent ductus arteriosus and a proposed update to the morphology classification system for dogs. *J Vet Intern Med*. 2018;32:648–657. https://doi.org/10.1111/jvim.15068